Power Amplification with IMPATT Diodes in Stable and Injection-Locked Modes

YOICHIRO TAKAYAMA

Abstract—The behavior of nonlinear power amplifiers using IMPATT diodes in both stable and injection-locked modes was investigated theoretically and experimentally. A method of graphical interpretation of the characteristics of negative-resistance diode amplifiers, based on the large-signal diode admittance chart, is presented. The characteristics of the simplified model of the reflection-type amplifier using an X-band Read-type IMPATT diode have been evaluated. The experimental results of power amplification using an X-band Si IMPATT diode in both stable and injection-locked modes under various circuit conditions are given. It was shown that nonlinearity of the IMPATT diode susceptance causes distortions in the amplification and injection-locking characteristics.

I. Introduction

MICROWAVE power amplifiers, including injection-locked ones, using new negative-resistance diodes, such as IMPATT diodes and Gunn-effect diodes, have been investigated by several authors [1]–[9].[1] Nonlinear characteristics of the power amplifiers using negative-resistance diodes have been analyzed by Hines [7] by means of a tunnel-diode-like device model. In the analysis, frequency dependence of diode admittance and nonlinear susceptance effects, which are present in IMPATT and Gunn-effect diodes, were not taken into consideration. Experimental investigations for injection-locked oscillators or amplifiers were carried out, so far, following Adler's theory [10], which is reliable only when the gain is large and the input small.

It is our purpose to obtain a basic understanding of the behavior of the reflection-type nonlinear amplifiers using negative-resistance diodes, especially IMPATT diodes, in both stable and injection-locked modes, and provide an available guide for the power amplifier design. A method of graphical interpretation was worked out for the characteristics of the nonlinear amplifiers using negative-resistance diodes. The method is based on the diode large-signal admittance chart, and is applicable not only to stable modes but also to injection-locked modes. The behavior of IMPATT-diode nonlinear power amplifiers was investigated theoretically and experimentally for both stable and injection-locked modes. The characteristics of the simplified model of the reflection-type amplifier using the X-band Read-type IMPATT diode were evaluated. In order to understand the amplifier behavior and to design the amplifier, it is important to know the diode admittance characteristics. The admittance of the packaged X-band IMPATT diode used for power-amplification experiments was measured, and the results of power amplification under various circuit conditions in both stable and injection-locked modes are reported.

Manuscript received April 12, 1971; revised July 6, 1971.

The author is with the Electron Device Research Laboratory, Central Research Laboratories, Nippon Electric Company, Ltd., 1753 Shimonumabe, Kawasaki, Japan.

[1] Since this paper was written, Schere [17] has published an analysis which gives some large-signal amplification characteristics of IMPATT-diode amplifiers in a stable mode.

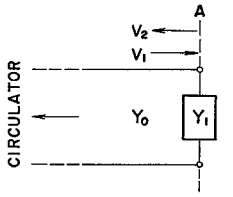

Fig. 1. Schematic diagram for a reflection-type amplifier.

II. Analytical Evaluation

A. Reflection-Type Amplifier

The reflection-type amplifier, in stable or injection-locked mode, makes use of a circulator for providing input–output isolation. The basic network used for analysis is shown in Fig. 1, where V_1 and V_2 are the incident and reflected voltage waves at reference plane A. The active network (whose admittance is Y_1), including the negative-resistance diode, is connected to the ideal lossless circulator through the ideal lossless transmission line of characteristic admittance Y_0. It is assumed that the diode terminal ac voltage is sinusoidal[2] and that stable solutions for steady-state single-frequency operations exist.

For the steady-state single-frequency operation, V_1 and V_2 can be expressed by

$$V_1 = \boldsymbol{V}_1 e^{j\omega t}$$
$$V_2 = \boldsymbol{V}_2 e^{j(\omega t+\phi)} \tag{1}$$

where ω is operating frequency, $\boldsymbol{V}_1$ and $\boldsymbol{V}_2$ are the amplitudes of V_1 and V_2, respectively, and ϕ is phase angle of V_2 with respect to V_1. Similarly, the ac voltage V_3 across Y_1 is given by

$$V_3 = \boldsymbol{V}_3 e^{j(\omega t+\theta)} \tag{2}$$

where $V_3 = V_1 + V_2$. Noting that

$$\frac{V_2}{V_1} = \frac{Y_0 - Y_1}{Y_0 + Y_1}$$

[2] This assumption is reasonable at least for our IMPATT diode amplifiers [11].

we obtain

$$\frac{V_3}{V_1} = \frac{2Y_0}{Y_0 + Y_1}. \tag{3}$$

Let us define the equivalent load admittance by

$$Y_2 = -Y_1 \tag{4}$$

where Y_2 satisfies the relation

$$\frac{V_1}{V_2} = \frac{Y_0 - Y_2}{Y_0 + Y_2}. \tag{5}$$

It is found that the normalized equivalent load admittance y_2 ($= Y_2/Y_0$) can be represented by

$$y_2 = g + jb$$

where

$$g = 1 - 2\alpha\cos\theta$$

$$b = 2\alpha\sin\theta$$

$$\alpha = V_1/V_3. \tag{6}$$

Eliminating θ, we obtain the locus of the equivalent load admittance in the admittance plane as follows:

$$(1-g)^2 + b^2 = (2\alpha)^2. \tag{7}$$

This is a circle with radius 2α centered on the point (1,0), and the phase angle θ as a parameter. Let us assume that

$$Y_1 = Y_d + Y_c$$

where the lossless resonant-circuit admittance Y_c is given by $Y_c = jB_c(\omega)$, and Y_d by $Y_d = G_d(\omega, V_3) + jB_d(\omega, V_3)$, which is the diode admittance under sinusoidal voltage drive. We can now express the relation between V_1 and V_3 by

$$\{g_d(\omega, V_3) + 1\}^2 + \{b_d(\omega, V_3) + b_c\}^2 = (2V_1/V_3)^2 \tag{8}$$

where $g_d = G_d/Y_0$, $b_d = B_d/Y_0$, and $b_c = B_c/Y_0$.

Power expressions are given by using the relations

$$P_1 = \tfrac{1}{2}Y_0V_1^2$$

$$P_2 = \tfrac{1}{2}Y_0V_2^2$$

$$P_g = \tfrac{1}{2}|G_d|V_3^2 \tag{9}$$

where P_1 and P_2 are input and output powers, respectively, and P_g is the diode generation power which is equal to $(P_2 - P_1)$.

We will give a graphical interpretation of the amplifier behavior by use of the diode admittance chart and the locus of the equivalent load admittance. The locus of the negative diode admittance $-y_d(V_3)$ at frequency ω_1, that of the negative diode admittance $-y_d(\omega)$ at ac voltage amplitude V_{30}, and that of $bc(\omega)+1$, are shown in Fig. 2(a), where $y_d = Y_d/Y_0$. The arrows indicate the directions of the increase of V_3 and ω. The circle whose center is on Q is a locus of an equivalent load admittance with $\alpha = \alpha_1$ at frequency ω_1. The point at which $V_3 \simeq 0$ is denoted by B, and the point at which $y_c = y_c(\omega_1)$ by Q.

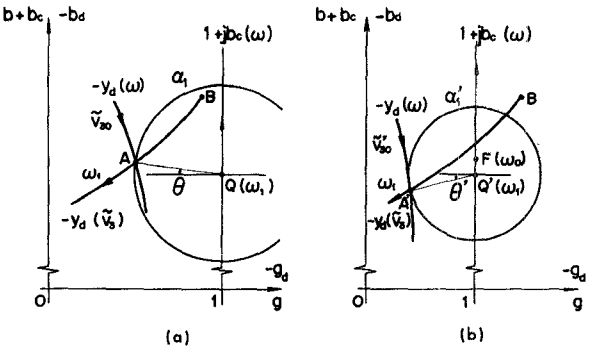

Fig. 2. Graphical explanation of amplifier behavior. (a) Stable mode. (b) Injection-locked mode.

θ is measured in the clockwise direction. It is assumed that there is no free-running operating point in Fig. 2(a). The intersection A gives a possible operating point where $\omega = \omega_1$, $V_1 = V_{10}(=\alpha_1 V_{30})$, and $V_3 = V_{30}$. θ is the phase angle of V_3 with respect to V_1. Similarly, the injection-locked operation is interpreted graphically in Fig. 2(b), where the free-running oscillation, whose operating point is F and frequency is ω_0, which is assumed to be different from ω_1, takes place without input signals. Generally, even in the stable mode it is possible that the locus of the diode admittance at a given frequency and the circle which is the locus of the equivalent load admittance intersect at two points. In an ordinary situation of the injection-locked mode, the higher voltage-amplitude point or the smaller phase-difference point is stable. However, both operating points can be stable in certain cases. The conditions for stable operation are discussed in the Appendix.

Shift of the operating point on the diode admittance chart takes place by the variation of input power and/or operating frequency resulting from the dependence of diode admittance on ac voltage amplitude and operating frequency. The shift of the operating point gives rise to the variation of the radius of the circle of equivalent load admittance. In ordinary operation of negative-resistance diodes, such as IMPATT and Gunn-effect diodes, the negative diode conductance decreases and the power generation first increases, then decreases with an increase of ac voltage amplitude. In ordinary cases, but not always, with an increase of input power, the operating point at a given frequency shifts towards a smaller negative-diode conductance point. This corresponds to the increase of the radius of the equivalent load-admittance locus. Thus at higher input levels we see a decrease of gain, or output saturation, or a decrease of output power which is input plus generation power. It is also found that the input power level at which the same power generation is obtained increases with an increase of load conductance Y_0. This corresponds to an increase of the radius of the circle of equivalent load admittance.

Frequency response can be investigated in terms of shifting frequency ω_1. Asymmetry of the frequency response is related to the gradient of the loci of the diode

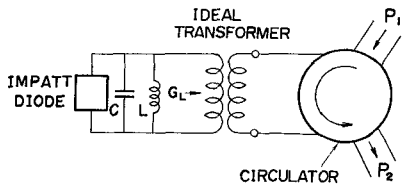

Fig. 3. Model circuit of the reflection-type IMPATT-diode amplifier.

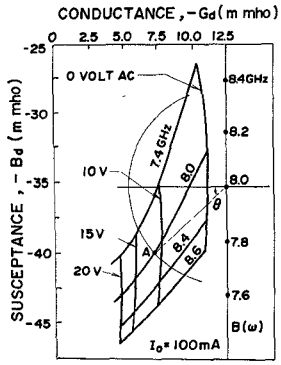

Fig. 4. Read-type IMPATT-diode admittance (7.4–8.6 GHz) [12] and equivalent-load admittance.

admittance at a given frequency and the diode admittance at a given ac voltage amplitude. Even in the stable mode, the gradient of the diode admittance locus at a given frequency can give two intersections with the circle which is the locus of the equivalent load admittance. In such a case, there are two operating points with the same gain at a given frequency, and a gain peak point appears on the input–output response curve with an increase of input power level.

B. Model

The results obtained are used for the calculation of some characteristics of the reflection-type IMPATT-diode amplifier. Fig. 3 shows a simple model for amplification using the X-band Read-type IMPATT diode whose large-signal admittance is based on the theoretically calculated characteristics by Scharfetter and Gummel [12]. An ideal transformer is used to adjust the load conductance G_L. The diode has a junction area 5×10^{-4} cm^2 and a depletion layer capacitance $C_d=9.5\times10^{-13}$F, the diode dc current being held at 100 mA. Fig. 4 shows the diode admittance chart (7.4~8.6 GHz) and the locus of an equivalent load admittance at frequency $f_1=8.0$ GHz.

The Q and the resonant frequency of the circuit, including C_d, are defined by the equations

$$Q_L = \omega_0(C + C_d)/G_L$$

$$\omega_0 = 2\pi f_0 = 1/\sqrt{L(C + C_d)}.$$

The amplification characteristics vary with circuit conditions. The circuit conditions chosen for the calculation of characteristics are given in Table I.

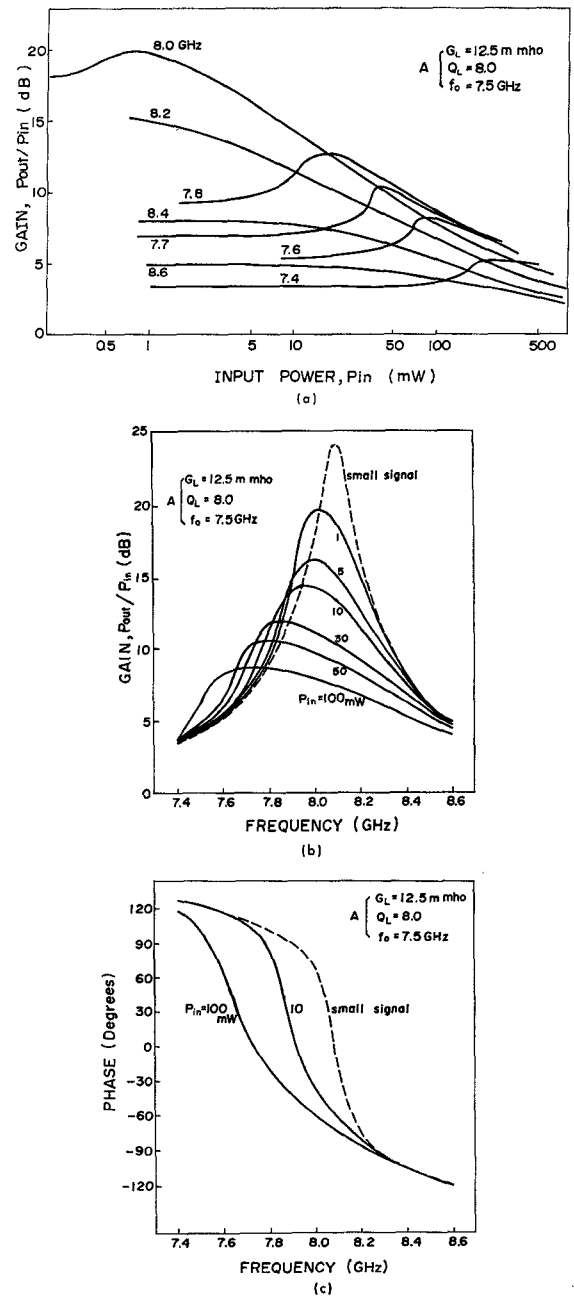

Fig. 5. Theoretical characteristics of the reflection-type amplifier model using the Read-type IMPATT diode under circuit conditions $G_L=12.5$ mmho, $Q_L=8.0$, and $f_0=7.5$ GHz. (a) Input–output responses. (b) Frequency responses. (c) Phase of output signal.

TABLE I
CIRCUIT CONDITIONS OF AMPLIFIER

	G_L(mmho)	Q_L	fo(GHz)
A	12.5	8.0	7.5
B	18.75	5.4	7.5

The results of numerical calculations are given in Figs. 5 and 6, where P_{in} and P_{out} are input and output power levels, respectively. Fig. 5(a) shows input–output responses at several frequencies, Figs. 5(b) and 6 show

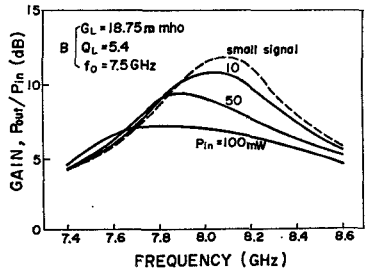

Fig. 6. Theoretical frequency responses of the reflection-type amplifier model using the Read-type IMPATT diode under circuit conditions $G_L = 18.75$ mmho, $Q_L = 5.4$, $f_0 = 7.5$ GHz.

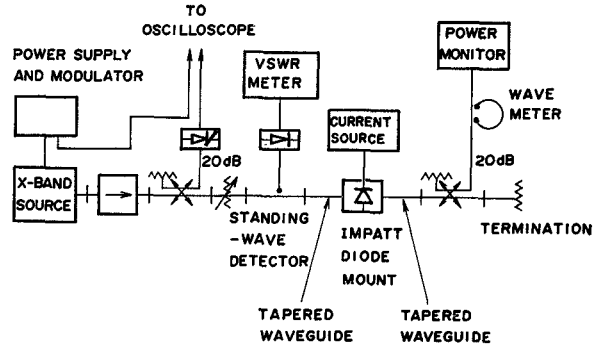

Fig. 7. Circuit for measuring the packaged diode admittance.

frequency responses for constant input power levels, and Fig. 5(c) shows the phase of the output signal at several input levels.

In Fig. 5(a) we see that at frequencies lower than 8 GHz, gain peak points appear with an increase of input power levels. In this case the locus of the given-frequency diode admittance and the circle of the equivalent-load admittance intersect at two points. It is seen from Fig. 5(a) that at smaller input levels the gain at lower frequencies is smaller than that at higher frequencies. However, the relation is reversed with the increase of input power levels. This corresponds to the shifts of gain peak points with the variation of input levels in Fig. 5(b) and 6. The characteristics for a relatively heavy load are shown in Fig. 6. These effects are primarily caused by the nonlinearity of the diode susceptance or the gradient of the locus of the diode admittance at a given frequency.

III. Experimental

Amplification experiments were carried out in X band using a packaged Si IMPATT diode (AD611C, NEC) imbedded in a waveguide 4.4 mm high. For the purpose of understanding the amplifier behavior and designing the amplifier, it is important to characterize the diode by measuring the admittance.

A. Packaged Diode Admittance

The circuit for measuring the packaged diode admittance is shown in Fig. 7. The reduced-height waveguide

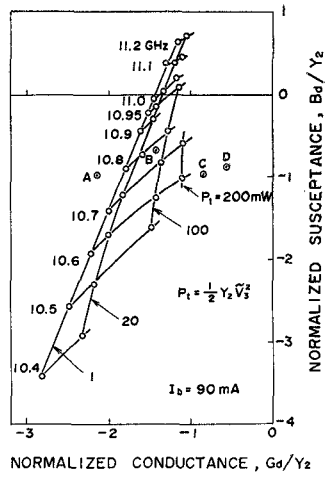

Fig. 8. Admittance of the packaged X-band IMPATT diode (AD611C, NEC) mounted in reduced-height waveguide, dc current is 90 mA.

mount is connected to standard X-band waveguides through tapered waveguide transformers. The sweep oscillator or reflex klystron provides the square-wave modulated signal for standing-wave measurements. The transmitted signal is monitored on the power meter. For the calibration of the power level, the detected pulse waveform is observed with an oscilloscope.

Fig. 8 shows the admittance characteristics of the packaged diode, whose conductance G_d and susceptance B_d are normalized by the characteristic admittance Y_2 of the reduced-height waveguide. The diode ac voltage amplitude V_3 is given by

$$V_3 = \sqrt{2P_t/Y_2}$$

where P_t is the transmitted power level.

The break-down voltage of the diode is 66.1 V and the junction capacitance is 0.68 pF. The diode dc current is 90 mA. We see in Fig. 8 that the packaged diode is in parallel resonance at about 11 GHz, and is inductive at frequencies lower than the resonant frequency. The diode is capacitive in itself. However, the packaged diode, which has parasitic elements arising from the inductance of the ribbon used to contact the semiconductor chip and the capacitance of the dielectric cylinder, changes to an inductive element. The series-resonant frequency at 1-mA dc current is 7.6 GHz. If we define packaged diode Q by means of

$$Q_d = \frac{\omega_0}{2|G_d|} \cdot \left.\frac{\partial B_d}{\partial \omega}\right|_{\omega_0}$$

then we have, as an example, $Q_d \simeq 14$ at $\omega_0 = 10.6$ GHz, $|G_d|/Y_2 = 1.44$, from Fig. 8. Q_d is essential to estimate the capability for broad-band amplification.

B. Amplification Experiments

The waveguide mount for the X-band reflection-type amplifier using the IMPATT diode is schematically shown in Fig. 9, which is the same as the main cavity of the

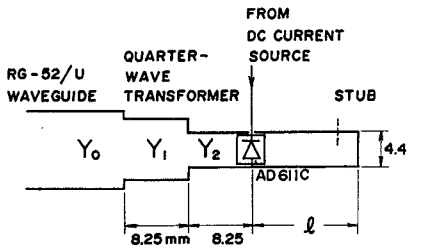

Fig. 9. Schematic structure of the reflection-type X-band IMPATT-diode amplifier.

TABLE II

CIRCUIT CONDITIONS UNDER WHICH THE IMPATT DIODE AMPLIFICATION MEASUREMENTS WERE CARRIED OUT

	fo (GHz)	P_0 (mW)	ℓ (mm)	h_1 (mm)	G_L/Y_2
A	10.85	0	10.5	10	2.16
B	10.76	167	10.5	8.0	1.45
C	10.89	321	12.5	6.7	0.86
D	10.55	355	12.5	5.0	0.59

highly stabilized oscillator [13]. The mount is connected to an X-band waveguide circulator through a quarter-wave transformer. Diode dc current, which is supplied through the RF choke, is held at 90 mA. The load conductance is adjusted with the transformer, and the frequency is tuned by a waveguide short or a stub. A spectrum analyzer is utilized for distinguishing the stable injection-locked operation. Amplification experiments were carried out in both stable and injection-locked modes under various circuit conditions, as shown in Table II. The load conductance was calculated at frequency f_0 at a reference plane placed on the diode position. The length of the waveguide short from the diode is l and the quarter-wave transformer height is h_1.

In case A in Table II, no oscillation takes place when undriven, and f_0 roughly represents the band-center frequency. In cases B, C, and D in Table II, free-running oscillations take place when undriven; f_0 represents the free-running frequency and P_0 the free-running output power. Undriven diode operating points for the cases in Table II are shown by points A, B, C, and D in Fig. 8. In case D, the free-running output power is maximum. The results of the amplification experiments are shown in Figs. 10–13. The amplification operation under the conditions in Table II (case A) is of a stable mode. The amplification operations under the conditions in Table II (cases B, C, and D) are of an injection-locked mode, where measurements were carried out over the stable-locked operating range. We see that the gain decreases and the bandwidth or locking range increases with the increase of load. Generation power versus input power in the injection-locked mode under the conditions in Table II (cases C and D) is shown in Fig. 14. We see a remarkable overdriving at higher input levels.

We can observe various nonlinear and frequency-de-

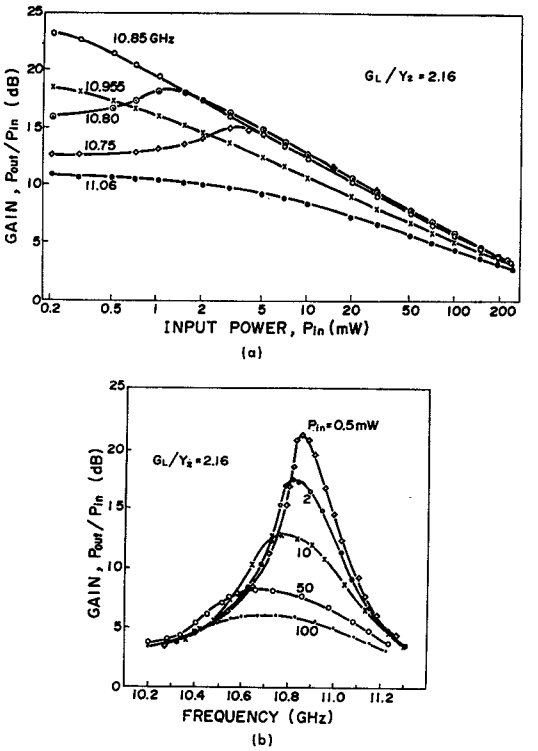

Fig. 10. Amplification characteristics in stable mode with $G_L/Y_2 = 2.16$. (a) Input–output responses. (b) Frequency responses.

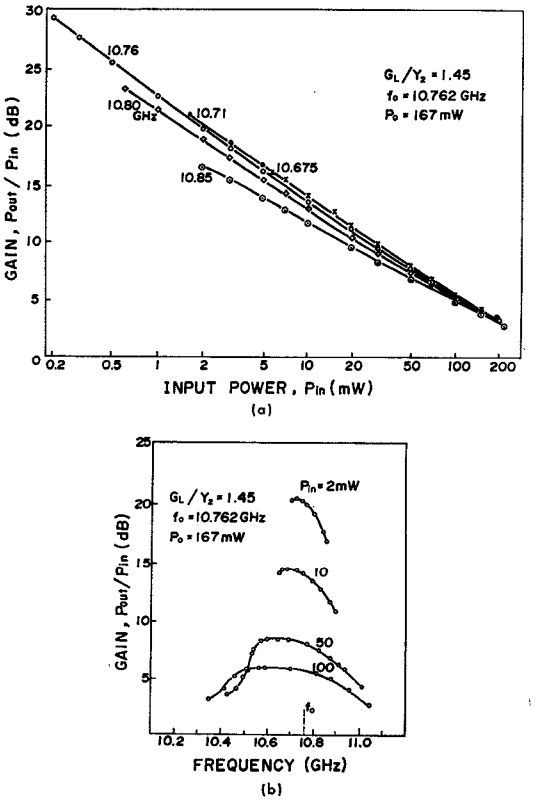

Fig. 11. Amplification characteristics in injection-locked mode with $G_L/Y_2 = 1.45$. (a) Input–output responses. (b) Frequency responses.

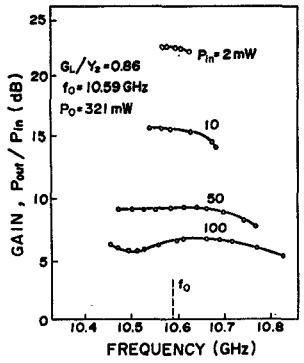

Fig. 12. Frequency responses in injection-locked mode with $G_L/Y_2=0.86$.

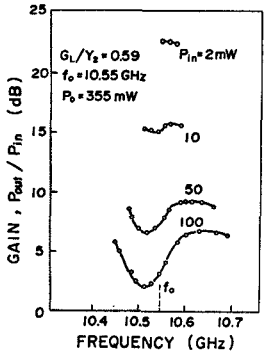

Fig. 13. Frequency responses in injection-locked mode with $G_L/Y_2=0.59$.

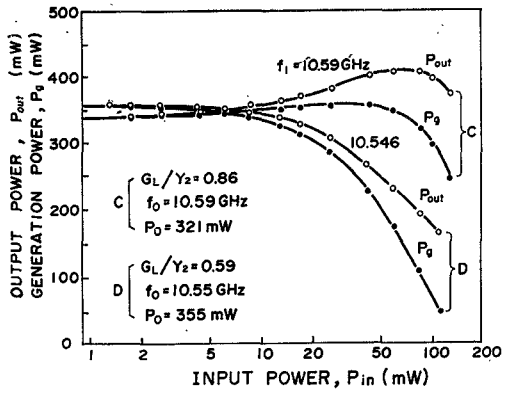

Fig. 14. Generation power versus input power in injection-locked mode.

pendent effects, such as power saturation, overdriving, gain peak frequency shift, and asymmetrical locking range, which can easily be explained from the diode admittance characteristics, if we neglect the frequency dependence of the characteristics of the quarter-wave transformer and apply the analysis and graphical interpretation.

IV. Conclusions

In order to attain an intuitive grasp of the behavior of the nonlinear power amplifiers using negative-resistance diodes, we have presented a method of the graphical interpretation of amplification characteristics. The method is applicable to both stable and injection-locked modes. The behavior of the nonlinear power amplifiers using IMPATT diodes in both stable and injection-locked modes have been investigated theoretically and experimentally. The characteristics of the simplified model of the reflection-type amplifier, using the X-band IMPATT diode, have been evaluated based on the diode large-signal admittance. Power amplification experiments were carried out using an X-band IMPATT diode in both stable and injection-locked modes. It was shown that nonlinearity of the IMPATT diode susceptance causes distortions in the amplification and injection-locking characteristics.

Appendix

The injection-locking stability criteria have been obtained by Kurokawa [14], and Okabe and Okamura [15]. Stable conditions are herewith derived in forms convenient for the discussion of the reflection-type amplifier in Fig. 1.

Assume that in (3) V_3 and ω are deviated slightly from the steady-state values V_{30} and ω_0, respectively. Then we can express the deviation of the normalized admittance $y_1(=Y_1/Y_0)$ as

$$\delta y = \left(\frac{\partial y_1}{\partial \omega}\right)_{\omega_0} \cdot (\omega - \omega_0) + \left(\frac{\partial y_1}{\partial V_3}\right)_{V_{30}} \cdot (V_3 - V_{30}). \tag{10}$$

In ac circuit theory, the time derivative corresponds to multiplication by $j\omega$. Referring to (3) we have

$$V_1 = \tfrac{1}{2}(1 + y_{10} + \delta y)V_3.$$

Thus we get

$$2\frac{V_1}{V_3}e^{-j\theta} = 1 + y_{10} + \left(\frac{\partial y_1}{\partial \omega}\right)\left(\frac{d\theta}{dt} - j\,\frac{1}{V_3}\cdot\frac{dV_3}{dt}\right) + \left(\frac{\partial y_1}{\partial V_3}\right)\delta V_3 \tag{11}$$

where $y_{10}=y_1$ at $\omega=\omega_0$, $V_3=V_{30}$, and $\delta V_3 = V_3 - V_{30}$. Using $\theta=\theta_0+\delta\theta$ and $e^{-j\delta\theta}\simeq 1-j\delta\theta$ for small deviation $\delta\theta$, multiplying (11) by $(\delta y_1/\partial\omega)^*$, and dividing the resulting equation into the real and imaginary parts, we obtain two differential equations for δV_3 and $\delta\theta$. Eliminating $\delta\theta$ from these equations, we obtain a differential equation for δV_3. If δV_3 decays with time, we have

$$\mathrm{Im}\left[\left\{V_{30}\left(\frac{\partial y_1}{\partial V_3}\right) + 4\alpha e^{-j\theta_0}\right\}\left(\frac{\partial y_1}{\partial \omega}\right)^*\right] < 0$$

$$\mathrm{Re}\left[\left\{V_{30}\left(\frac{\partial y_1}{\partial V_3}\right) + 2\alpha e^{-j\theta_0}\right\} 2\alpha e^{j\theta_0}\right] > 0 \tag{12}$$

where $\alpha = V_1/V_{30}$. These conditions are illustrated in the complex plane for $2\alpha e^{-j\theta_0}$ in Fig. 15 as done by Fukatsu [16]. If $2\alpha e^{-j\delta_0}$ for the possible operating point given by

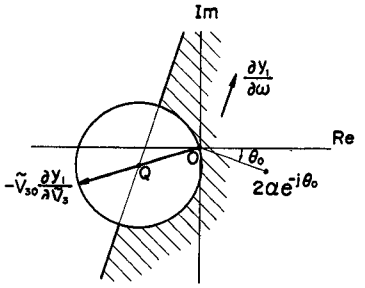

Fig. 15. Stability diagram in the complex plane for $2_{\alpha e}{}^{-j\theta_0}$. Shaded region gives stable operation.

(3) in Section II is in the shaded region in Fig. 15, then the point is a stable operating point. The shaded region is bounded by the straight line which is parallel to the vector $[\partial y_1/\partial\omega]$ through the point Q and the circle whose center is on Q and radius $\frac{1}{2}V_{30}\left|\partial y_1/\partial V_3\right|$. Point Q is the terminal point of the vector $-\frac{1}{2}V_{30}\partial y_1/\partial V_{30}$, whose original point is 0. Phase angle θ is measured in the clockwise direction.

As described in Section II, the diode admittance locus at a given frequency and the circle which is the locus of the equivalent load admittance intersect at two points under certain circumstances. Therefore, there can be two possible operating points. We see that, in the injection-locked mode $[\partial g_1/\partial V_3>0,\ g_1=\mathrm{Re}\ y_1<0]$, the higher voltage-amplitude point or the smaller phase-difference point is stable, but that both possible operating points can be stable under certain circumstances.

Acknowledgment

The author wishes to thank Dr. K. Ayaki and S. Nagano for their encouragement and suggestions, H. Kondo for supplying diode mounts and measuring junction capacitance and series-resonant frequency, and Dr. H. Murakami for his kind interest.

References

[1] B. C. DeLoach and R. L. Johnston, "Avalanche transit-time microwave oscillators and amplifiers," *IEEE Trans. Electron Devices* (*Special Issue on Semiconductor Bulk-Effect and Transit-Time Devices*), vol. ED-13, p. 181–186, Jan. 1966.

[2] F. Ivanek and V. G. K. Reddi, "*X*-band oscillator and amplifier experiments using avalanche diode periodic structures," in *1969 Int. Solid-State Circuits Conf., Dig. of Papers*, p. 80.

[3] E. F. Scherer and M. J. Barrett, "A broadband multistage avalanche amplifier at *X*-band," in *1969 Int. Solid-State Circuits Conf., Dig. of Papers*, p. 82.

[4] L. D. Armstrong, "GaAs IMPATT diodes, oscillators and amplifiers," in *G-MTT 1970 Int. Microwave Symp., Dig. Tech. Papers*, p. 279.

[5] D. M. Snider, "A one watt CW, 20% efficient *X*-band avalanche diode amplifier," in *G-MTT 1970 Int. Microwave Symp., Dig. Tech. Papers*, p. 285.

[6] M. E. Hines, "*X*-band power amplification using Gunn effect diodes," *Proc. IEEE* (Lett.), vol. 56, pp. 1590–1591, Sept. 1968.

[7] ——, "Negative-resistance diode power amplification," *IEEE Trans. Electron Devices*, vol. ED-17, pp. 1–8, Jan. 1970.

[8] B. S. Perlman and R. E. Marx, "Linear microwave solid state transferred electron power amplifiers with a large gain-bandwidth product," in *G-MTT 1970 Int. Microwave Symp., Dig. Tech. Papers*, p. 227.

[9] T. Isobe and M. Tokita, "A new microwave amplifier for multichannel FM signals using an IMPATT diode oscillator," in *1969 Int. Solid-State Circuits Conf., Dig. of Papers*, p. 26.

[10] R. Adler, "A study of locking phenomena in oscillators," *Proc. IRE*, vol. 34, pp. 351–357, June 1946.

[11] J. W. Gewartowski and J. E. Morris, "Active IMPATT diode parameters obtained by computer reduction of experimental data," *IEEE Trans. Microwave Theory Tech.*, vol. MTT-18, pp. 157–161, Mar. 1970.

[12] D. L. Scharfetter and H. K. Gummel, "Large-signal analysis of a silicon Read diode oscillator," *IEEE Trans. Electron Devices*, vol. ED-16, pp. 64–77, Jan. 1969.

[13] S. Nagano and H. Kondo, "Highly stabilized half-watt IMPATT oscillator," *IEEE Trans. Microwave Theory Tech.* (*Special Issue on Microwave Circuit Aspects of Avalanche Diode and Transferred Electron Devices*), vol. MTT-18, pp. 885–890, Nov. 1970.

[14] K. Kurokawa, "Some basic characteristics of broadband negative resistance oscillator circuits," *Bell Syst. Tech. J.*, vol. 48, pp. 1937–1955, July–Aug. 1969.

[15] Y. Okabe and S. Okamura, "Analysis of stability and noise of oscillators in free-running, synchronized-running and parallel-running," *Trans. Inst. Electron. Commun. Eng.* (Japan), vol. 52-B, pp. 755–762, Dec. 1969.

[16] Y. Fukatsu, presented at the 1970 Joint Conv. For Inst. Electrical Engineers (Japan), *Symp. Rec.*, Paper S. 14-4, p. 13.

[17] E. F. Scherer, "Large-signal operation of avalanche-diode amplifiers," *IEEE Trans. Microwave Theory Tech.* (*Special Issue on Microwave Circuit Aspects of Avalanche-Diode and Transferred Electron Devices*), vol. MTT-18, pp. 922–932, Nov. 1970.